## A Lightweight Protocol for Matchgate Fidelity Estimation

Jędrzej Burkat<sup>1,\*</sup> and Sergii Strelchuk<sup>2</sup>

<sup>1</sup>Cavendish Laboratory, Department of Physics, University of Cambridge, Cambridge CB3 0US, UK

<sup>2</sup>Department of Computer Science, University of Oxford, Oxford OX1 3QD, UK

We present a low-depth randomised algorithm for the estimation of entanglement fidelity between an n-qubit matchgate circuit  $\mathcal U$  and its noisy implementation  $\mathcal E$ . Our procedure makes use of a modified Pauli-Liouville representation of quantum channels, with Clifford algebra elements as a basis. We show that this choice of representation leads to a block-diagonal compound matrix structure of matchgate superoperators which enables construction of efficient protocols for estimating the fidelity, achieving a  $1/\sqrt{n}$  speedup over protocols of Flammia & Liu [PRL 106, 230501]. Finally, we offer simple extensions of our protocol which (without additional overhead) benchmark matchgate circuits intertwined by Clifford circuits, and circuits composed of exclusively nearest-neighbour  $XY(\theta)$  gates or Givens rotations – forming the first known method for direct benchmarking of matchgate subgroups.

### I. INTRODUCTION

Implementing quantum computation is a complex and challenging process due to the ubiquitous presence of noise and decoherence. Accurately identifying the magnitude of these effects leads to the development of more efficient error mitigation strategies thus leading to better utilization of existing quantum hardware.

Matchgates [1–6] (MGs) represent an important family of two-qubit gates for quantum computation, forming an intriguing class of computations analogous to the dynamics of (non-interacting) free fermions, which are classically efficiently simulable. Similarly to the well-studied case of Clifford computations, matchgate circuits are classically simulable in polynomial time, however with the addition of a SWAP gate, their computational power is lifted to universal quantum computation. Unlike Clifford gates, they form an infinite, continuous (Lie) group of operators that can be implemented natively on a range of architectures via the Mølmer-Sørensen procedure [7] and forms key primitives in superconducting quantum computing [8–11]. They have also made appearance in other architectures [12, 13].

The continuous nature of matchgate circuits makes the study of their behavior under realistic noise and decoherence conditions extraordinarily challenging – and in many cases outright impossible. So far, two methods [14, 15] have been devised for experimentally estimating their fidelities, both relying on the exponential fitting of data from large-depth circuits to characterise their average noise behaviour. Notably, these approaches struggle with circuits composed of exclusively  $XY(\theta)$  gates – also known as anisotropic Heisenberg spin coupling [16] or the XY interaction. Such gates fall into the category of matchgates, forming a subgroup of the matchgate group.

We present an efficient protocol for fidelity estimation, similar in spirit to a widely used procedure by S. Flammia & Y. Liu [17] and offering a  $1/\sqrt{n}$  speedup when applied to matchgate circuits. We first establish key mathematical results, working in a modified Pauli-Liouville (PL) representation of quantum channels. We then show that in this picture, it is experimentally straightforward to estimate the superoperator matrix overlap of two channels using only Pauli state preparation and measurement. Our procedure avoids issues with  $XY(\theta)$  gates, and may be extended to allow the benchmarking of matchgate circuits intertwined by arbitrary, distinct Clifford unitaries. Finally, we consider the fSim gate as an example – if parametrised to represent a matchgate, our method offers a speedup in estimating its fidelity. Outside of this parameter regime, it performs on par with [17]. The algorithm is easy to implement in practice and the work therein has the potential to greatly simplify the process of calibrating matchgate circuits for use in quantum computation.

### II. PRELIMINARIES

Channel Fidelity. Algorithms for estimating channel fidelity represent a key component of a variety of practical quantum information processing protocols. Channel fidelity describes the average overlap between pure states  $|\psi\rangle\langle\psi|$  acted on by an idealised channel  $\mathcal{U}$  (with a unitary matrix U), and the same state acted on by a (possibly noisy) quantum channel  $\mathcal{E}$ . Mathematically, it is defined as [18]:

$$F(\mathcal{E}, \mathcal{U}) = \int d\psi \langle \psi | U^{\dagger} \mathcal{E}(|\psi\rangle \langle \psi|) U | \psi \rangle$$
$$= \frac{dF_e(\mathcal{E}, \mathcal{U}) + 1}{d+1}. \tag{1}$$

where  $d\psi$  is the uniform Haar measure over  $\mathcal{H}$ , normalised so that  $\int d\psi = 1$ , and d is the Hilbert space dimension.  $F_e(\mathcal{E}, \mathcal{U})$  is the entanglement fidelity – a closely related and experimentally accessible quantity. Estimating it is the modus operandi of many randomised benchmarking protocols, as it allows for the

<sup>\*</sup> jbb55@cam.ac.uk

direct calculation of  $F(\mathcal{E}, \mathcal{U})$  by Equation (1).

Pauli-Liouville (PL) Representation. In the PL picture of quantum channels, we consider the vector space  $\mathbb{C}^{2^n \times 2^n}$  spanned by the complex matrices  $W_i \cong |i\rangle$ , with the Hilbert-Schmidt inner product  $\langle\langle i|j\rangle\rangle = 2^{-n}\mathrm{Tr}(W_i^\dagger W_j)$ . Under this representation, both pure and mixed quantum states may be written as  $\rho = \sum_i \rho_i W_i$ , or (using double ket notation) as  $|\rho\rangle\rangle = \sum_i \rho_i |i\rangle\rangle$ . The action of unitary operators, as well as CPTP maps, can then be represented through multiplication by  $2^{2n} \times 2^{2n}$  superoperator, or process matrices. Multiplication of vectors by superoperators  $\hat{\Lambda}$  corresponds to the application of a quantum channel, whereas multiplying superoperator matrices gives a composition of quantum channels:

$$\widehat{\Lambda \circ \Omega} |\rho\rangle\rangle = |\Lambda(\Omega(\rho))\rangle\rangle = \widehat{\Lambda}\widehat{\Omega} |\rho\rangle\rangle. \tag{2}$$

In a given basis, the superoperators can be written as:

$$\hat{\Lambda} = \sum_{i,j=1}^{2^{2n}} \chi_{\Lambda}(i,j)|i\rangle\rangle\langle\langle j|, \qquad (3)$$

with the matrix elements given by:

$$\chi_{\Lambda}(i,j) = \frac{1}{2^n} \text{Tr}(W_i^{\dagger} \Lambda(W_j)). \tag{4}$$

Our protocol will make use of the *Clifford basis*, a set of  $2^{2n}$  orthonormal monomials of Clifford algebra generators  $c_i$ , the latter forming a set of 2n Hermitian matrices satisfying the anti-commutation relations:

$$\{c_i, c_j\} = 2\delta_{ij}\mathbb{1}, \quad i, j \in [2n]. \tag{5}$$

Up to unitary equivalence, the generators can be chosen to be the Jordan-Wigner operators:

$$c_{2k-1} = Z \otimes \cdots \otimes Z \otimes X \otimes \mathbb{1} \otimes \cdots \otimes \mathbb{1}$$

$$c_{2k} = \underbrace{Z \otimes \cdots \otimes Z}_{k-1} \otimes Y \otimes \underbrace{\mathbb{1} \otimes \cdots \otimes \mathbb{1}}_{n-k}.$$
(6)

We will denote elements of this basis as  $c_I = c_{i_1} \dots c_{i_{|I|}}$ , where  $I \subseteq \{1, \dots, 2n\}$  is a set of lexicographically ordered indices taken from [2n], with  $c_{\emptyset} = \mathbb{1}$  (an example of our ordering can be seen in Figure 3). In the Jordan-Wigner representation every basis element is proportional to a Pauli string:

$$c_I = \phi_I \mathbb{P}_I, \tag{7}$$

and for any subset  $I \subseteq [2n]$  with cardinality k the Hermitian conjugate is given by  $c_I^{\dagger} = (-1)^{k(k-1)/2}c_I$ . As a result, the phase  $\phi_I$  is either  $\pm 1$  or  $\pm i$ , and remains real or pure imaginary across all monomials indexed by subsets with constant degree k (see Appendix A). The difference between Clifford and Pauli bases then amounts to a re-ordering of the basis elements and change of

phase – a subtle alteration which considerably simplifies the protocol.

Matchgate PL Superoperators. Matchgates (also known as Fermionic Linear Optics gates) are two-qubit operators – denoted G(A,B) – acting as  $A \in U(2)$  on the odd-parity  $\{|01\rangle, |10\rangle\}$ , and  $B \in U(2)$  on the even-parity  $\{|00\rangle, |11\rangle\}$  subspaces of  $\mathbb{C}^2 \otimes \mathbb{C}^2$ :

$$G(A,B) = \begin{pmatrix} a_{11} & 0 & 0 & a_{12} \\ 0 & b_{11} & b_{12} & 0 \\ 0 & b_{21} & b_{22} & 0 \\ a_{21} & 0 & 0 & a_{22} \end{pmatrix}, \tag{8}$$

such that  $\det A = \det B$ . Operators of this form for which  $\det A \neq \det B$  (for example, a SWAP or CZ gate) are denoted  $\tilde{G}(A, B)$ .

Any match gate circuit (MGC) may be written as a Gaussian operation  $U = e^{-iH}$ , where

$$H = i \sum_{i \neq j} h_{ij} c_i c_j \tag{9}$$

is a quadratic Hamiltonian, with the coefficients  $h_{ij}$  forming a real, antisymmetric  $2n \times 2n$  matrix. Previous work [1, 3–5] has shown that the orthogonal SO(2n) matrix  $R = e^{4h}$  generated from h provides full information about U. Furthermore, conjugating a generator  $c_i$  by a matchgate unitary U is a rotation by R in the space of Clifford algebra generators:

$$Uc_i U^{\dagger} = \sum_{j=1}^{2n} R_{ji} c_j. \tag{10}$$

This relation suggests that the Clifford basis is a natural choice for the Pauli-Liouville representation of matchgate unitaries. It turns out that the associated process matrices  $\hat{\mathcal{U}}$  in this basis can be easily calculated, requiring only the knowledge of R.

**Theorem 1.** For any matchgate circuit  $U = e^{-iH}$  with an associated SO(2n) matrix R, in the Clifford algebra generator basis the superoperator matrix elements  $\chi_{\mathcal{U}}(I,J)$  are given by:

$$\chi_{\mathcal{U}}(I,J) = \delta_{|I|,|J|} \det |R_{I,J}| \tag{11}$$

where  $R_{I,J}$  is a submatrix of R for which each  $i^{th}$  row  $i \in I$  is preserved, and each  $j^{th}$  column  $j \in J$  is preserved. Consequently,  $\hat{\mathcal{U}}$  is a block diagonal matrix with 2n+1 blocks, each of which is a  $\binom{2n}{k} \times \binom{2n}{k}$  compound matrix  $C_k(R)$ , where k is the degree of the monomial  $c_I = c_{i_1} \dots c_{i_k}$ .

*Proof.* This is a known and straightforward result (see [19], for example). Starting with the definition of  $\chi_U(I,J)$ , we can prove it by inserting  $\mathbb{1} = U^{\dagger}U$  between each  $c_j$  operator:

$$\chi_{\mathcal{U}}(I,J) = \frac{1}{2^{n}} \operatorname{Tr} \left( (c_{i_{1}} \dots c_{i_{m}})^{\dagger} U(c_{j_{1}} \dots c_{j_{k}}) U^{\dagger} \right) \\
= \frac{1}{2^{n}} \operatorname{Tr} \left( (c_{i_{1}} \dots c_{i_{m}})^{\dagger} Uc_{j_{1}} U^{\dagger} \dots Uc_{j_{k}} U^{\dagger} \right) \\
= \frac{1}{2^{n}} \operatorname{Tr} \left( (c_{i_{1}} \dots c_{i_{m}})^{\dagger} \sum_{\substack{\nu_{1}, \dots, \nu_{k} \\ \nu_{1} \neq \dots \neq \nu_{k}}} R_{\nu_{1}j_{1}} \dots R_{\nu_{k}j_{k}} c_{\nu_{1}} \dots c_{\nu_{k}} \right) \\
= \frac{1}{2^{n}} \operatorname{Tr} \left( (c_{i_{1}} \dots c_{i_{m}})^{\dagger} \sum_{\substack{0 \leq \nu_{1} < \dots < \nu_{k} \leq 2n, \\ \sigma \in S_{k}}} \operatorname{sgn}(\sigma) R_{\nu_{\sigma(1)}j_{1}} \dots R_{\nu_{\sigma(k)}j_{k}} c_{\nu_{1}} \dots c_{\nu_{k}} \right) \\
= \delta_{mk} \sum_{\sigma \in S_{k}} \operatorname{sgn}(\sigma) R_{i_{\sigma(1)}j_{1}} R_{i_{\sigma(2)}j_{2}} \dots R_{i_{\sigma(k)}j_{k}} \\
= \delta_{mk} \det |R_{(j_{1}\dots j_{k}, j_{1}\dots j_{k})}|. \quad \Box$$

### Matchgate Circuit Fidelity Estimation: Requirements and Runtime

Inputs:

- Matchgate circuit  $\mathcal{E}$  for an idealised unitary  $\mathcal{U}$ , with the ability to prepare and measure Pauli eigenstates.
- Clasically pre-computed superoperator matrix  $\hat{\mathcal{U}}$  with elements  $\chi_{\mathcal{U}}(I,J)$ .
- (Optional) Well-conditioning parameter  $\alpha$ , such that for all (I, J), either  $|\chi_{\mathcal{U}}(I, J)| \ge \alpha$  or  $|\chi_{\mathcal{U}}(I, J)| = 0$ .

Output:

• Entanglement fidelity estimator  $\tilde{Y}$ , for which  $F_e(\mathcal{E}, \mathcal{U})$  lies in the range  $[\tilde{Y} - 2\epsilon, \tilde{Y} + 2\epsilon]$  with probability at least  $1 - 2\delta$ .

Runtime Parameters (without  $\mathcal{E}$  with well-conditioning):

• Sample number:

$$l = \left\lceil \frac{1}{\epsilon^2 \delta} \right\rceil, \left\lceil \frac{2 \ln(2/\delta)}{\alpha^2 \epsilon^2} \right\rceil$$

• Iteration number:

$$m_{\mu} = \left[ \frac{2\ln(2/\delta)}{\chi_{\mathcal{U}}(I_{\mu}, J_{\mu})^2 l\epsilon^2} \right]$$

• Total shot bound:

$$m \leq \mathcal{O}(\frac{1}{\epsilon^2 \delta} + \frac{2^{2n} \ln(1/\delta)}{\sqrt{n}\epsilon^2}), \ \mathcal{O}(\frac{\ln(1/\delta)}{\alpha^2 \epsilon^2})$$

For any  $\hat{\mathcal{U}}$  with PL matrix elements  $\chi_{\mathcal{U}}(I,J)$ :

$$m \le \mathcal{O}(\frac{1}{\epsilon^2 \delta} + \frac{\#[\chi_{\mathcal{U}}(I,J) \ne 0]}{2^{2n}} \frac{\ln(1/\delta)}{\epsilon^2})$$

For comparison, the superoperator matrices for Clifford gates in this basis are monomial matrices, i.e. unitaries with exactly one non-zero entry in each row and column equal to  $\pm 1$  or  $\pm i$ . If the Clifford is also a matchgate (like in the case of iSWAP), the process matrix becomes block-diagonal again, with each block being an orthogonal monomial matrix (i.e. a signed permutation matrix in  $B(m) \subset SO(m)$ ).

Most importantly, Theorem 1 tells us that in the PL representation a matchgate superoperator can have at most  $\sum_{k=0}^{2n} \binom{2n}{k}^2 = \binom{4n}{2n}$  elements. Asymptotically, this upper bounds of the number of non-zero elements as:

$$\#[\chi_{\mathcal{U}}(I,J) \neq 0] < 2^{4n}/\sqrt{n}.$$
 (13)

### III. MATCHGATE FIDELITY ESTIMATION

Let  $\mathcal{U}$  be a unitary channel (with an associated superoperator matrix  $\hat{\mathcal{U}}$ ) describing the evolution of an n-qubit input state under the application of a matchgate circuit U, and  $\mathcal{E}$  the mathematical description of its actual, noisy implementation. We assume the ability to either prepare and measure states in the Pauli eigenbasis or apply single-qubit unitaries out of  $\{X, H, S\}$  onto the  $|0\rangle$  state with negligible error (which itself may be characterised using other methods first), and wish to quantify the distance between  $\mathcal{U}$  and  $\mathcal{E}$ . A natural measure for this is the entanglement fidelity, which can be calculated from the superoperator matrix overlap:

$$F_{e}(\mathcal{E}, \mathcal{U}) = \frac{1}{2^{2n}} \operatorname{Tr}(\hat{\mathcal{U}}^{\dagger} \hat{\mathcal{E}})$$

$$= \frac{1}{2^{2n}} \sum_{i,j,k,l} \chi_{\mathcal{U}}^{*}(i,j) \chi_{\mathcal{E}}(k,l) \langle \langle i|k \rangle \rangle \langle \langle l|j \rangle \rangle$$

$$= \frac{1}{2^{2n}} \sum_{i,j} \chi_{\mathcal{U}}^{*}(i,j) \chi_{\mathcal{E}}(i,j). \tag{14}$$

To estimate the entanglement fidelity for matchgate circuits, we propose the following: first, pick pairs of indices (I, J) at random with probabilities  $\Pr(I, J) = 2^{-2n}|\chi_{\mathcal{U}}(I, J)|^2$  and then determine matrix elements  $\chi_{\mathcal{E}}(I, J)$ , thus constructing the random variable:

$$X = \frac{\chi_{\mathcal{E}}(I, J)}{\chi_{\mathcal{U}}(I, J)},\tag{15}$$

which satisfies  $\mathbb{E}[X] = F_e(\mathcal{E}, \mathcal{U})$ . For the case of matchgates, by Equation (12) all superoperator matrix elements are real, and vanishing whenever  $|I| \neq |J|$ . Thus, Equation (14) may be rewritten as:

$$F_e(\mathcal{E}, \mathcal{U}) = \frac{1}{2^{2n}} \sum_{k=0}^{2n} \sum_{|I|=|J|=k} \chi_{\mathcal{E}}(I, J) \chi_{\mathcal{U}}(I, J). \quad (16)$$

Before applying our algorithm, one must isolate the matrix  $R=e^{4h}$  associated with the matchgate circuit and compute superoperator elements by taking the appropriate matrix minors. The elements of h may be computed from  $h_{ij}=2^{-n}\mathrm{Tr}((c_ic_j)^{\dagger}\log U)$ . Key information concerning our protocol provided on the previous page and Algorithm 1. Proofs are relegated to Appendix B.

Expectation Values. To illustrate why our protocol works, we follow similar reasoning to [17]. We consider the 'perfect' random variable X, as in (15), which may be averaged to reveal the entanglement fidelity. We define an estimator  $Y = \frac{1}{l} \sum_{\mu} X_{\mu}$ , where l is the 'sample number' and  $X_{\mu}$  is the  $\mu^{\text{th}}$  sample of X, obtained by randomly choosing a pair of indices  $(I_{\mu}, J_{\mu})$  (cf. step 1). In expectation,  $\mathbb{E}(Y) = \mathbb{E}(X_{\mu}) = F_e(\mathcal{E}, \mathcal{U})$ , as the expectation value of  $X_{\mu}$  over the random choices of  $(I_{\mu}, J_{\mu})$  is given by:

$$\mathbb{E}(X_{\mu}) = \sum_{\mu} \frac{\chi_{\mathcal{E}}(I_{\mu}, J_{\mu})}{\chi_{\mathcal{U}}(I_{\mu}, J_{\mu})} \frac{\chi_{\mathcal{U}}(I_{\mu}, J_{\mu})^{2}}{2^{2n}}$$

$$= F_{e}(\mathcal{E}, \mathcal{U}).$$
(17)

Because we cannot directly measure the matrix elements  $\chi_{\mathcal{E}}(I_{\mu}, J_{\mu})$ , each  $X_{\mu}$  must be approximated with an estimator  $\tilde{X}_{\mu}$ , obtained from performing  $m_{\mu}$  'iterations' of a random circuit (steps 3–5) and averaging the collected data (step 6). Equation (19) shows that over measurement outcomes, the quantity  $B_{\mu\nu}$  (constructed in step 5) averages to  $\chi_{\mathcal{E}}(I_{\mu}, J_{\mu})$ . Therefore, the expectation value of each  $\tilde{X}_{\mu}$  is:

$$\mathbb{E}(\tilde{X}_{\mu}) = \frac{\chi_{\mathcal{E}}(I_{\mu}, J_{\mu})}{\chi_{\mathcal{U}}(I_{\mu}, J_{\mu})} = X_{\mu}. \tag{18}$$

Finally, we define a third estimator  $\tilde{Y} = \frac{1}{l} \sum_{\mu} \tilde{X}_{\mu}$ , which satisfies  $\mathbb{E}(\tilde{Y}) = Y$  and is experimentally accessible through steps 1-7. Algorithm 1 may thus be seen as

the composition of two successive estimations, returning an estimate  $\tilde{Y}$  of Y. In turn, Y is an estimate of the entanglement fidelity. Thus, in expectation we have:

$$\mathbb{E}_{\mu}[\mathbb{E}_{\nu}(\tilde{Y})] = \mathbb{E}_{\mu}(Y) = F_{e}(\mathcal{E}, \mathcal{U}).$$

# Algorithm 1: Matchgate Circuit Fidelity

for  $\mu$  in range(l):

1. Select a pair of index subsets  $(i_1 \dots i_k, j_1 \dots j_k)_{\mu} = (I_{\mu}, J_{\mu})$  at random, each with probability:

$$\Pr(I,J) = \frac{1}{2^{2n}} \left( \chi_{\mathcal{U}}(I,J) \right)^2.$$

2. Convert the corresponding Clifford monomials into Pauli operators as:

$$(c_{i_1} \dots c_{i_k})^{\dagger}_{\mu} = \phi_{I_{\mu}}^* \mathbb{P}_{I_{\mu}},$$
  
$$(c_{j_1} \dots c_{j_k})_{\mu} = \phi_{J_{\mu}} \mathbb{P}_{J_{\mu}},$$

and store the product of phases as  $\phi_{\mu} = \phi_{I_{\mu}}^* \times \phi_{J_{\mu}} = \pm 1$ .

for  $\nu$  in range  $(m_{\mu})$ :

- 3. Pick an eigenstate  $|\lambda_{\mu\nu}\rangle$  of  $\mathbb{P}_{J_{\mu}}$  at random (with probability  $1/2^n$ ) and prepare it, storing its eigenvalue as  $\lambda_{\mu\nu} = \pm 1$ .
- 4. Apply the matchgate circuit  $\mathcal{E}$ .
- 5. Make a measurement  $\mathbb{P}_{I_{\mu}}$  in the Pauli basis to obtain a bitstring  $\mathbf{c}$ , and compute  $A_{\mu\nu} = (-1)^{|\mathbf{c}|}$ . Multiply this by the eigenvalue and phase to obtain

$$B_{\mu\nu} = A_{\mu\nu}\lambda_{\mu\nu}\phi_{\mu} = \pm 1.$$

6. Compute the estimator  $\tilde{X}_{\mu}$ :

$$\tilde{X}_{\mu} = \frac{1}{\chi_{\mathcal{U}}(I_{\mu}, J_{\mu})m_{\mu}} \sum_{\nu=1}^{m_{\mu}} B_{\mu\nu}.$$

7. Compute the estimator  $\tilde{Y}$ :

$$\tilde{Y} = \frac{1}{l} \sum_{\mu=1}^{l} \tilde{X}_{\mu}$$

$$= \sum_{\mu=1}^{l} \sum_{\nu=1}^{m_{\mu}} \frac{A_{\mu\nu} \lambda_{\mu\nu} \phi_{\mu}}{\chi_{\mu}(I_{\mu}, J_{\mu}) m_{\mu} l}.$$

return  $\tilde{Y}$ 

$$\mathbb{E}(B_{\mu\nu}) = \sum_{k=1}^{2^n} \frac{1}{2^n} \lambda_{\mu\nu}^{(k)} \phi_{\mu} \left( \Pr(A_{\mu\nu}^{(k)} = +1) - \Pr(A_{\mu\nu}^{(k)} = -1) \right)$$

$$= \frac{\phi_{\mu}}{2^n} \sum_{k=1}^{2^n} \lambda_{\mu\nu}^{(k)} \operatorname{Tr} \left( \mathbb{P}_{I_{\mu}}^{\dagger} \mathcal{E}(|\lambda_{\mu\nu}^{(k)}\rangle\langle\lambda_{\mu\nu}^{(k)}|) \right)$$

$$= \frac{\phi_{\mu}}{2^n} \operatorname{Tr} \left( \mathbb{P}_{I_{\mu}}^{\dagger} \mathcal{E}(\mathbb{P}_{J_{\mu}}) \right)$$

$$= \chi_{\mathcal{E}}(I_{\mu}, J_{\mu}).$$
(19)

Steps 3–5 (repetitions over  $\nu$ ) bring  $\tilde{Y}$  to within  $\pm \epsilon$  of Y (with failure probability  $\delta$ ), whereas taking samples of  $\tilde{X}_{\mu}$  (repetitions over  $\mu$ ) brings Y  $\epsilon$ -close to  $F_{e}(\mathcal{E}, \mathcal{U})$ . Overall, we obtain an estimate of the entanglement fidelity with a probability  $1-2\delta$  of lying within  $\pm 2\epsilon$  of its true value.

Well-Conditioning. We give two bounds for l: one for the general case, where no assumption is made about the structure of  $\hat{\mathcal{U}}$  or the size of its elements, and another for the case where  $|\chi_{\mathcal{U}}(I,J)| \geq \alpha$  for all non-zero elements. The latter is the 'well-conditioning' property from [17]. Whilst it is true that all Clifford gates are well-conditioned (with  $\alpha=1$ ), a matchgate circuit can correspond to an arbitrarily small rotation with a small value of  $\alpha$ . However, determining  $\alpha$  in particular instances of MGCs can be done efficiently, thanks to the compound matrix structure of  $\hat{\mathcal{U}}$ . Guidance on how  $\alpha$  may be found for an arbitrary matchgate circuit is given in Appendix C. Essentially, this makes use the fact that any  $R \in SO(2n)$  can be decomposed into a product of n(2n-1) 2D rotations with generalised Euler angles.

### IV. COMPARISON TO EXISTING METHODS

Prior to our work, two methods for benchmarking matchgates have been published; one due to J. Claes et al [15], and the other due to J. Helsen et al [14]. The two methods are similar in their approach, making use of the group structure of nearest-neighbour G(A, B) gates via randomised benchmarking (RB). This is achieved by repeated preparation of random circuits, with random elements of the matchgate group applied at variable circuit depths. After collecting measurements, data is polynomially fitted to extract error parameters  $\lambda$ , which are then used to estimate the fidelity of the gate set. These approaches assume that the gate noise being measured is independent of the particular gates  $U \in G$  applied, i.e. constant across the matchgate group (when this assumption is relaxed, the deviations from the gateindependent noise model are supressed, so the resulting noise information may still be seen as an average). Comparisons between the three methods are given in Table 1.

A recent addition to the literature is the work of A. Chapman and S. Flammia [20], which proposes an efficient method for learning parameters of group-averaged, gate-dependent noise channels for collections of matchgates. Similarly to RB-based methods this approach utilises matchgate twirling and consequently returns average channel parameters, although the noise is allowed to vary between different group elements.

In contrast, our procedure allows one to directly benchmark each instance of U without averaging over G. It does not require polynomial fitting to estimate the relevant error parameters - the entanglement fidelity estimate  $F_e(\mathcal{E},\mathcal{U})$  is given directly from the constructed Y. However, it has lower robustness to SPAM noise, though only Pauli state preparation and measurement are required. We believe this method is advantageous in its simplicity and speed, and will benefit practicioners who wish to benchmark gates at some particular parameter  $\theta$ , for example the  $XX(\theta)$  or  $XY(\theta)$  gates in the context of calibration. Finally, if  $\alpha$  is identified for a particular instance of the MGC, then the shot number bound is no longer dependent on system size n, opening up the possibility of fast benchmarking of matchgate circuits on many qubits.

### A. Decay parameters $\lambda$ and the fidelity

Despite the apparent differences between RB-based techniques and our work, the guiding principles are similar. The goal of randomised benchmarking is to identify the average fidelity of a constant (or average) error channel  $\mathcal{E}$ :

$$F(\mathcal{E}) = F(\mathcal{E}, \mathbb{1}) = \frac{2^n F_e(\mathcal{E}, \mathbb{1}) + 1}{2^n + 1}.$$
 (20)

The entanglement fidelity  $F_e(\mathcal{E}, \mathbb{1})$  is then the trace of the error channel:

$$F_e(\mathcal{E}, \mathbb{1}) = \frac{1}{2^{2n}} \text{Tr}(\hat{\mathcal{E}}).$$
 (21)

	Present Work	HNRW'20	CRW'20					
Outcome:	$F(\mathcal{E},\mathcal{U})$ : the fidelity between $\mathcal{U}$	The fidelity $F(\mathcal{E})$ of the ave	The fidelity $F(\mathcal{E})$ of the average error channel $\mathcal{E}$ , acting as					
	and its noisy implementation $\mathcal{E}$ .	$\mathcal{E} \circ \mathcal{U}$ on all MGC channels $\mathcal{U}$ . Gives the bound $F(\mathcal{E} \circ \mathcal{U}) \leq F(\mathcal{U})$						
Assumptions:	Noiseless Pauli basis SPAM	Robust against SPAM noise.						
	(State Preparation and Measurement).	Assumes a gate-independent noise channel $\mathcal{E}$ .						
Applied	Matchgate circuit,	Matchgate circuits with Haar random						
Gates:	Pauli SPAM.	$R \in SO(2n)$ , Pauli SPAM.						
Noise	PL Superoperator elements $\chi_{\mathcal{E}}(I,J)$ :	Decay parameters $\lambda_k$ , $k \in [2n]$ :						
Parameters:	$\chi_{\mathcal{E}}(I,J) = \operatorname{Tr}(c_I^{\dagger}\mathcal{E}(c_J))/2^n.$							
	$F_e(\mathcal{E}, \mathcal{U}) = 2^{-2n} \sum_{I,J} \chi_{\mathcal{U}}^*(I,J) \chi_{\mathcal{E}}(I,J).$	$F_e(\mathcal{E}) = 2^{-2}$	$\sum_{k=0}^{2n} {2n \choose k} \lambda_k.$					
Noise	Prepare random eigenstates of $c_J$ ,	2n+1 polynomial	n polynomial fittings					
Parameter	apply the channel ${\mathcal E}$ and measure	fittings of	of $f_k(N) = \sum_{l=1}^2 C_{kl} \lambda_{kl}^N$ ,					
Estimation:	in the $c_I^{\dagger}$ basis. Repeat many times.	$f_k(N) = C_k \lambda_k^N.$	one fitting of $f_0(N) = C_0 \lambda_0^N$ .					
Procedure:	Algorithm 1.	(i) Pick $k \in [2n]$ (or $k \in [n]$ ). (ii) Prepare a Pauli eigenstate,						
		apply $\mathcal{O}(N)$ randomly sampled MGs, measure in Pauli basis.						
		(iii) Repeat (ii) $M$ times. (iv) Repeat (ii) - (iii) for different $N$ .						
		(v) Repeat (i) - (iv) for different $k$ . (vi) Compute functions $\hat{f}_k(N)$						
		from measurement data, and polynomially fit to find the decay						
		parameters $\lambda_k$ . (vii) Estimate $F(\mathcal{E})$ using Equation (22).						
Runtime	l samples (choices of SPAM basis),	$2n+1$ values of $k \in [2n]$ ,	$n+1$ values of $k \in [n]$ ,					
Parameters:	$m_{\mu}$ iterations (random circuit	repetitions $M$ ,	repetitions $M$ ,					
	repetitions).	sequence lengths $N$ .	sequence lengths $N$ .					
Shot Scaling:	$m \le \mathcal{O}(1/\epsilon^2 \delta + 2^{2n} \ln(1/\delta)/\sqrt{n}\epsilon^2)$	No analytic bounds provided.						
Benchmarking	No protocol modifications required	Benchmark $XX(\theta)$ gates via $XX(\theta) = XY(\theta/2)X_1XY(\theta/2)X_1$ ,						
XY Gates:		Assume $X_1$ is noiseless and $XY(\theta/2)$ noise is multiplicative.						

FIG. 1. Comparison of Matchgate Benchmarking protocols.  $F_e(\mathcal{E}, \mathcal{U})$  and  $F_e(\mathcal{E}) = F_e(\mathcal{E}, \mathbb{1})$  are the entanglement fidelities, related to channel fidelity via Equation (1)

The authors of [14] make use of projection matrices  $\{\hat{P}_k\}$ , which project onto the invariant subspaces  $\{\Gamma_k\}$  of irreducible representations of the matchgate group. Inserting  $\sum_{k=0}^{2n} P_k = 1$  into the above, we get:

$$\frac{1}{2^{2n}}\operatorname{Tr}(\hat{\mathcal{E}}) = \frac{1}{2^{2n}} \sum_{k=0}^{2n} \operatorname{Tr}(\hat{P}_k \hat{\mathcal{E}})$$

$$= \frac{1}{2^{2n}} \sum_{k=0}^{2n} {2n \choose k} \lambda_k, \qquad (22)$$

where:

$$\lambda_k = \frac{\text{Tr}(\hat{P}_k \hat{\mathcal{E}})}{\text{Tr}(\hat{P}_k)} = \frac{1}{\binom{2n}{k}} \text{Tr}(\hat{P}_k \hat{\mathcal{E}}).$$
 (23)

The subspaces projected onto by  $\hat{P}_k$  are exactly the block-diagonals of  $\hat{\mathcal{U}}$  as described in Theorem 1. Comparing our expression to Equation (16), we can relate the decay parameters  $\lambda_k$  to the partial sums:

$$\lambda_{k}' = \frac{1}{\binom{2n}{k}} \sum_{|I|=|J|=k} \chi_{\mathcal{E}}(I,J) \chi_{\mathcal{U}}(I,J)$$
$$= \frac{1}{\binom{2n}{k}} \operatorname{Tr}(\hat{P}_{k} \hat{\mathcal{U}}^{\dagger} \hat{\mathcal{E}})$$
(24)

which evaluate to  $F_e(\mathcal{E}, \mathcal{U})$  through Equation (22). Our procedure finds 'gate-specific' decay parameters  $\lambda_k'$ , which encode information about the fidelity between a particularly chosen MGC and its noisy implementation. This is in contrast to the decay parameters of [14, 15, 20] which characterise the noise channel under a matchgate twirl.

### B. The XY Group

Despite their technical sophistication, RB-based approaches tend to struggle with subgroups of the matchgate group (for example,  $XY(\theta)$  gates or Givens rotations). In general, the group formed by matchgate circuits has irreps appearing with multiplicities, which complicate identifying the decay parameters  $\lambda_k$ .

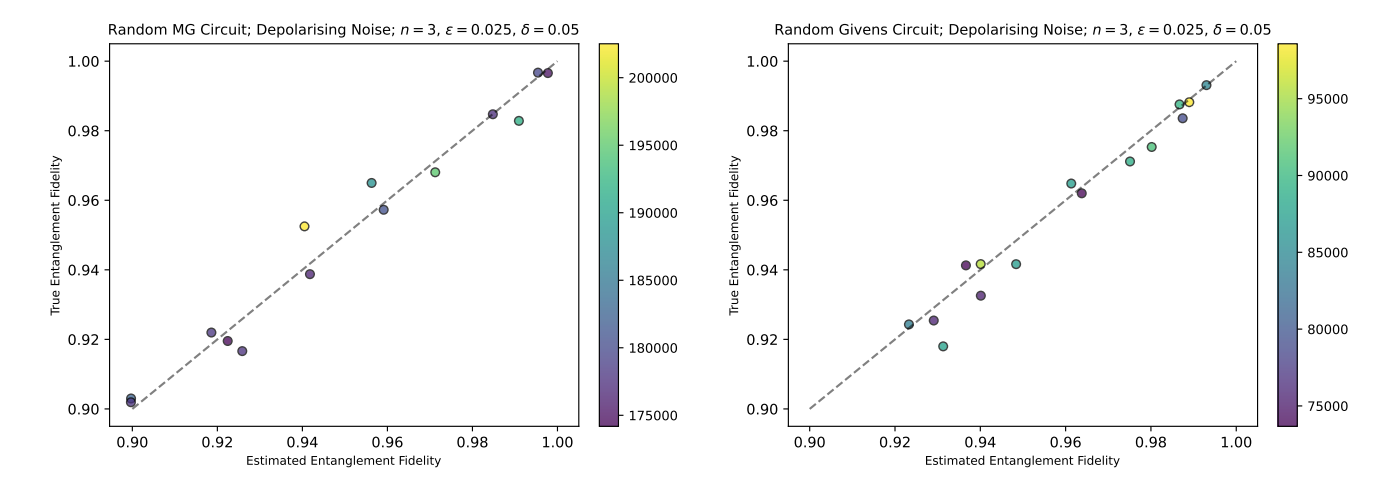


FIG. 2. Simulation of Algorithm 1 for n=3 Qubits. Each point is the output of Algorithm 1 applied to a Haar-randomly sampled circuit followed by an n-qubit depolarising channel. Colour maps indicate shot numbers in each run. Restricting to nearest-neighbour Givens rotations is seen to decrease the shot number by about 1/2, in agreement with Section IVB. Code used to simulate our algorithm is provided in [21].

The authors of [14] avoid this issue by expanding the group to include a bit-flip X on the final qubit, obtaining a multiplicity-free decomposition. then propose benchmarking  $XY(\theta)$  gates indirectly, by preparing XX gates through  $XX(\theta) = XY(\theta/2)(X \otimes$  $\mathbb{1}XY(\theta/2)(X\otimes\mathbb{1})$ , and assuming that (i) the singlequbit gates are noiseless and (ii) the noise from the XYgates is multiplicative. On the other hand, the method in [15] handles multiplicaties directly by fitting functions of  $a_k$  degree-N polynomials  $\sum_{i}^{k} C_{ij} \lambda_{ij}^{N}$  (where  $a_k$  is the multiplicity of the  $k^{\text{th}}$  irrep) to the data. For the matchgate group, these multiplicites are at most 2, though for the XY subgroup they grow with the qubit number n. The authors find that because of this scaling, their proposed method of multiplicity benchmarking fails for the XY group – so neither is feasible for a direct fidelity estimation of  $XY(\theta)$  gates exclusively.

In contrast, our method is able to benchmark  $XY(\theta)$  circuits without additional difficulty with a moderately faster runtime compared to general MGCs. This is because for such circuits, the rotation matrix R takes the form (under reshuffling of rows and columns):

$$R \cong \tilde{R} \oplus \tilde{R}', \quad \tilde{R} \in SO(n),$$
 (25)

where  $\tilde{R}'_{ij} = (-1)^{i+j} \tilde{R}_{ij}$ . Thus, the original matrix R is block-diagonal (with a sparsity reduction of a half), and we expect the full superoperator  $\hat{\mathcal{U}}$  to have roughly half as many non-zero elements (leading to a reduction of the expected number of shots, cf. Equation (B7)). Similarly, if U is a circuit of nearest-neighbour Givens rotations, R will take the form:

$$R = \tilde{R} \otimes \mathbb{1}_2, \quad \tilde{R} \in SO(n).$$
 (26)

These observations follow from considering the quadratic Hamiltonians of nearest-neighbour XY gates and Givens rotations, and the structure of the  $\mathfrak{so}(2n)$  Lie algebra generators they correspond to. Importantly, in both cases (and any other where R belongs to some subgroup of SO(2n)) the effect of the sparsity reduction in R leads to a constant decrease in shot number, on top of the  $1/\sqrt{n}$  speedup for matchgate circuits.

# V. BEYOND MATCHGATES: BENCHMARKING CLIFFORD + MG + CLIFFORD CIRCUITS

Our protocol may also be used (without additional overhead) to benchmark circuits of the form  $W = V_1 \circ U \circ V_2$ , where U is a matchgate and  $V_1, V_2$  are arbitrary Clifford circuits. Because Clifford unitaries form monomial superoperator matrices, one can calculate  $\hat{W}$  directly and proceed with the same instructions ( $\hat{W}$  will have entries from  $\hat{U}$  permuted and multiplied by a phase from  $\{\pm 1, \pm i\}$ , preserving its sparsity). However, if  $\hat{U}$  has already been calculated then this is not necessary. For the new circuit, pairs of  $c_{I'}, c_{J'}$  are sampled using the probability distribution

$$\Pr(I', J') = 2^{-2n} (\operatorname{Tr}(c_{I'}^{\dagger} V_2 U V_1 c_{J'} V_1^{\dagger} U^{\dagger} V_2^{\dagger}))^2,$$

which is equal to the original distribution  $\Pr(I,J)$  for  $c_I = V_2^{\dagger} c_{I'} V_2$  and  $c_J = V_1 c_{J'} V_1^{\dagger}$ . Hence, we may use the original probability distribution, and upon sampling I,J calculate  $c_{I'} = V_2 c_I V_2^{\dagger}$ ,  $c_{J'} = V_1^{\dagger} c_J V_1$ . In the  $c_{I'}$  basis the superoperator elements remain invariant:

$$\chi_{\mathcal{W}}(I', J') = \frac{1}{2^n} \operatorname{Tr}(c_{I'}^{\dagger} V_2 U V_1 c_{J'} V_1^{\dagger} U^{\dagger} V_2^{\dagger})$$

$$= \frac{1}{2^n} \operatorname{Tr}(c_I^{\dagger} U c_J U^{\dagger})$$

$$= \chi_{\mathcal{U}}(I, J). \tag{27}$$

Because the dashed operators are also strings of Paulis, we may estimate  $\chi_{\mathcal{E}}(I',J')$  by preparing eigenstates of  $c_{J'}$ , applying  $\mathcal{W}$ , and measuring in the  $c_{I'}$  basis. This is effectively a passive transformation on the original algorithm, introducing no further computational cost other than identifying the new Pauli strings  $c_{I'}$  and  $c_{J'}$  (which may be done efficiently using stabilizer simulation methods). This is summarised by the following modification of Algorithm 1:

2\*. If the MGC is preceded by a Clifford circuit V<sub>1</sub> and succeeded by another Clifford circuit V<sub>2</sub>, the Clifford monomials are converted into Pauli operators as:

$$V_2 c_I^{\dagger} V_2^{\dagger} = \phi_{I_{\mu}}^* \mathbb{P}_{I_{\mu}}, \quad V_1^{\dagger} c_J V_1 = \phi_{J_{\mu}} \mathbb{P}_{J_{\mu}}.$$

The rest of the algorithm proceeds as before.

Interestingly,  $V_1UV_2$  need not be a MGC or a Clifford unitary for the modification to work. However, in a more general case of MGCs intertwined by Clifford circuits of the form  $W = V_1U_1V_2U_2\cdots U_kV_{k+1}$  the argument will not hold, unless it is possible to 'commute out' the  $V_i$ 's to the left and right of the  $U_i$ 's.

# VI. EFFICIENT MATCHGATE TOMOGRAPHY

So far, we have discussed the compound matrix structure of  $\hat{\mathcal{U}}$  in the context of verifying the action of matchgate unitaries. The superoperator structure of MGCs also makes learning about them easier. Suppose we are given a black box unitary circuit – which we can apply as many times as we like – with the promise that it is composed of nearest-neighbour matchgates only. In the general case, learning about the circuit is exponentially hard in the number of qubits, requiring full gate tomography. In the matchgate case the circuit is fully characterised by its SO(2n) matrix R, and an estimate of its  $4n^2$  elements gives complete information about U. By Theorem 1, these matrix elements are precisely  $\chi_{\mathcal{U}}(i,j)$  for  $i,j \in [2n]$ :

$$R_{ij} = \frac{1}{2^n} \text{Tr}(c_i^{\dagger} U c_j U^{\dagger}).$$

We can estimate the  $R_{ij}$ 's using steps 3–5 of Algorithm 1. This is the Linear Optics Tomography algorithm of [22]. We may use it to find the quadratic Hamiltonian elements:

$$\tilde{h}_{ij} = \frac{1}{4} \log(\tilde{R})_{ij},$$

from which the estimate  $\tilde{U}=e^{-i\tilde{H}}$  is computed by Equation (9). The authors of [22] show that to obtain  $\|\tilde{U}-U\|_{\diamond} \leq \epsilon$  with failure probability  $\delta, m = \mathcal{O}(n^3 \ln(n/\delta)/\epsilon^2)$  repetitions are sufficient.

#### VII. EXAMPLES

### A. Google's $fSim(\theta, \phi)$ gate

One may use our algorithm to benchmark the fidelity of Google's [8]  $fSim(\theta, \phi)$  gates, consisting of a power-ofiSWAP (MG) and controlled phase (non-MG) parts:

$$fSim(\theta, \phi) = \begin{pmatrix} 1 & 0 & 0 & 0\\ 0 & \cos \theta & -i \sin \theta & 0\\ 0 & -i \sin \theta & \cos \theta & 0\\ 0 & 0 & 0 & e^{i\phi} \end{pmatrix}.$$
(28)

When the latter is applied with  $\phi=0$ , the  $\mathrm{fSim}(\theta,0)$  operation is an  $XY(\theta)$  gate. However, when  $\phi\neq 0$  it becomes a  $\tilde{G}(A,B)$  gate with a process matrix which is no longer block diagonal. Whilst one may benchmark the  $\mathrm{fSim}(\theta,0)$  and  $\mathrm{fSim}(0,\phi)$  gates separately, our method still allows a full benchmark in one sweep – at the cost of a slightly higher expected shot count than before, dependent on the nonzero element count of the superoperator matrix (cf. Appendix B). We calculate the sparsity to equal  $94/256 \sim 37\%$ , giving a bound on the expected value of m to be:

$$\mathbb{E}(m) \le 1 + \frac{1}{\epsilon^2} (1/\delta + 47 \ln(4/\delta)/2).$$

Furthermore, if  $\phi = \pi$  (so that  $fSim(0, \pi)$  is a CNOT), by the discussion of Section V this bound decreases. The full superoperator matrix is given in Figure 3.

### B. Numerical Simulations

We provide data from noisy simulations of our protocol in Figure 2. In order to model average-to-worst case scenarios, random matchgate circuits were generated by sampling  $R \in SO(2n)$  out of the Haar distribution, from which the unitary and process matrices  $U, \hat{\mathcal{U}}$  were calculated. For each choice, random Pauli SPAM circuits were generated following Algorithm 1 and simulated using Qiskit Aer to collect data. Upon each application of U, a noise channel followed. To model noise we used an all-qubit depolarising channel (additional simulations with all-qubit amplitude damping and all-qubit amplitude + phase damping are available in [21]). Different choices of  $\epsilon, \delta$  affected the average shot counts, which we found to lie well below the

derived bounds. In particular, benchmarking circuits of exclusively nearest-neighbour Givens rotations led to the lowest shot counts, in agreement with Section IVB. The same speed-up also applies to nearest-neighbour  $XY(\theta)$  circuits. Our plots compare the estimated entanglement fidelity  $F_e(\mathcal{E},\mathcal{U})$  to the true value – we find that despite the seemingly high analytic scaling, the number of repetitions required to achieve a good estimate is comparable to the other approaches (which reported  $\mathcal{O}(10^5)$  shots for n=2,3 qubits [14, 15]).

Python code and Jupyter notebooks used in our simulations are available in [21].

#### ACKNOWLEDGMENTS

We thank Oscar Watts and Christopher Long for feedback on the manuscript, as well as various conference referees for their helpful comments. SS acknowledges support from the Royal Society University Research Fellowship and "Quantum simulation algorithms for quantum chromodynamics" grant (ST/W006251/1) and EPSRC Reliable and Robust Quantum Computing grant (EP/W032635/1).

### Appendix A: Properties of the Clifford Basis

To prove (7), we first note that all Clifford generators are by definition Hermitian. Consider a Clifford monomial  $c_I = c_{i_1} c_{i_2} \cdots c_{i_k}$  of degree k, and take its Hermitian conjugate:

$$c_I^{\dagger} = c_{i_k} \cdots c_{i_2} c_{i_1}. \tag{A1}$$

As the generators all anticommute, we can bring this expression back into the original order by performing a sequence of transpositions, each of which introduces a minus sign. This requires (k-1) transpositions for  $c_{i_k}$ , (k-2) transpositions for  $c_{i_{k-1}}$ , and so on, the total number being the sum of an arithmetic sequence. Hence,  $c_I^{\dagger} = (-1)^{k(k-1)/2} c_I$ . It follows that each element of the Clifford basis is either Hermitian or antihermitian, and this depends on whether k(k-1)/2is even or odd. Starting with k = 0 the transposition count forms the sequence of triangular numbers  $(0,0,1,3,6,10,\ldots)$ , so with increasing k the basis elements with |I| = k switch parity every two steps. That we can always write  $c_I$  as in (7) follows from the definition of the Jordan-Wigner representation, however the above also implies that  $\phi_I \times \phi_J = \pm 1$  so long as |I| = |J|, a fact we implicitly use in step 2 of Algorithm 1.

### Appendix B: Runtime Parameters

Here we derive expressions for the sample and iteration numbers  $l, m_{\mu}$  required for our protocol. These

closely follow the derivations in [17] with some minor amendments, but we include them for completeness.

#### 1. General Case

Bound 1. As discussed in the main text, we first wish to bound Y to lie  $\epsilon$ -close to the fidelity with probability  $1 - \delta$ :

$$\Pr(|Y - F_e(\mathcal{E}, \mathcal{U})| \ge \epsilon) \le \delta.$$
 (B1)

Much like in [17], we can bound the variance of each  $X_n$ :

$$\operatorname{Var}(X_{\mu}) = \mathbb{E}(X_{\mu}^{2}) - \mathbb{E}(X_{\mu})^{2}$$

$$= \sum_{\mu} 2^{-2n} \chi_{\mathcal{E}}(I_{\mu}, J_{\mu})^{2} - F_{e}(\mathcal{E}, \mathcal{U})^{2}$$

$$= F_{e}(\mathcal{E}, \mathcal{E}) - F_{e}(\mathcal{E}, \mathcal{U})^{2} < 1.$$
(B2)

It follows that  $\mathrm{Var}(Y) \leq 1/l,$  so we use Chebyshev's inequality:

$$\Pr(|Y - \mathbb{E}(Y)| \ge \frac{\lambda}{\sqrt{l}}) \le \frac{1}{\lambda^2},$$
 (B3)

with  $\delta = 1/\sqrt{\lambda}$  and  $l = \lceil 1/\epsilon^2 \delta \rceil$ .

Bound 2. We now wish to find the sample numbers  $m_{\mu}$ , such that  $\tilde{Y}$  is close to Y:

$$\Pr(|\tilde{Y} - Y| \ge \epsilon) \le \delta.$$
 (B4)

To do this, we use Hoeffding's inequality:

$$\Pr(|\tilde{Y} - \mathbb{E}(\tilde{Y})| \ge \epsilon) \le 2e^{-2\epsilon^2/C},$$
 (B5)

Where  $\tilde{Z}_{\mu\nu}$  are summands in  $\tilde{Y} = \sum_{\mu,\nu} \tilde{Z}_{\mu\nu}$  (cf. step 7) bounded as  $a_{\mu\nu} \leq \tilde{Z}_{\mu\nu} \leq b_{\mu\nu}$ , and  $C = \sum_{\mu,\nu} (b_{\mu\nu} - a_{\mu\nu})^2$ . Each  $\tilde{Z}_{\mu\nu}$  satisfies  $|\tilde{Z}_{\mu\nu}| \leq 1/\chi_{\mathcal{U}}(I_{\mu}, J_{\mu})m_{\mu}l$ , therefore

$$C = \sum_{\mu=1}^{l} \sum_{\nu=1}^{m_{\mu}} \frac{4}{\chi_{\mathcal{U}}(I_{\mu}, J_{\mu})^{2} m_{\mu}^{2} l^{2}}$$

$$= \sum_{\mu=1}^{l} \frac{4}{\chi_{\mathcal{U}}(I_{\mu}, J_{\mu})^{2} m_{\mu} l^{2}}.$$
(B6)

Thus, choosing  $m_{\mu} = \lceil 2 \ln(2/\delta)/\chi_{\mathcal{U}}(I_{\mu}, J_{\mu})^2 l \epsilon^2 \rceil$  ensures that the RHS of (B5) equals to  $\delta$ .

Bound 3. Finally, we bound the total number of shots  $m = \sum_{\mu=1}^{l} m_{\mu}$ . To do this, we bound the expected value  $\mathbb{E}(m)$ . By Markov's inequality, the actual number m needed for the stated  $\epsilon, \delta$  will be unlikely to differ from the expectation by much. First, we bound  $\mathbb{E}(m_{\mu})$ :

$$\mathbb{E}(m_{\mu}) = \sum_{\mu} \Pr(I_{\mu}, J_{\mu}) m_{\mu}$$

$$\leq \sum_{\mu} \Pr(I_{\mu}, J_{\mu}) \left( 1 + \frac{4 \ln(4/\delta)}{\chi_{\mathcal{U}}(I_{\mu}, J_{\mu})^{2} l \epsilon^{2}} \right)$$

$$\leq 1 + \frac{1}{2^{2n}} \sum_{\mu} \frac{4 \ln(4/\delta)}{l \epsilon^{2}}.$$
(B7)

	(0)	(1)	(2)	(3)	(4)	(12)	(13)	(14)	(23)	(24)	(34)	(123)	(124)	(134)	(234)	(1234)
(0)	1	0	0	0	0	0	0	0	0	0	0	0	0	0	0	0
(1)	0	$\cos \theta \cos^2 \frac{\phi}{2}$	$-\frac{1}{2}\cos\theta\sin\phi$	$\frac{1}{2} \sin \theta \sin \phi$	$\sin \theta \cos^2 \frac{\phi}{2}$	0	0	0	0	0	0	$-\frac{1}{2}i\sin\theta\sin\phi$	$i \sin \theta \sin^2 \frac{\phi}{2}$	$i \cos \theta \sin^2 \frac{\phi}{2}$	$\frac{1}{2}i\cos\theta\sin\phi$	0
(2)	0	$\frac{1}{2}\cos\theta\sin\phi$	$\cos \theta \cos^2 \frac{\phi}{2}$	$-\sin\theta\cos^2\frac{\phi}{2}$	$\frac{1}{2} \sin \theta \sin \phi$	0	0	0	0	0	0	$-i \sin \theta \sin^2 \frac{\phi}{2}$	$-\frac{1}{2}i\sin\theta\sin\phi$	$-\frac{1}{2}i\cos\theta\sin\phi$	$i \cos \theta \sin^2 \frac{\phi}{2}$	0
(3)	0	$\frac{1}{2} \sin \theta \sin \phi$	$\sin \theta \cos^2 \frac{\phi}{2}$	$\cos \theta \cos^2 \frac{\phi}{2}$	$-\frac{1}{2}\cos\theta\sin\phi$	0	0	0	0	0	0			$-\frac{1}{2}i\sin\theta\sin\phi$		0
(4)	0	$-\sin\theta\cos^2\frac{\phi}{2}$	$\frac{1}{2} \sin \theta \sin \phi$	$\frac{1}{2}\cos\theta\sin\phi$	$\cos \theta \cos^2 \frac{\phi}{2}$	0	0	0	0	0	0	$-\frac{1}{2}i\cos\theta\sin\phi$	$i \cos \theta \sin^2 \frac{\phi}{2}$	$-i \sin \theta \sin^2 \frac{\phi}{2}$	$-\frac{1}{2}i\sin\theta\sin\phi$	0
(12)	0	0	0	0	0	$\cos^2 \theta$	$-\sin\theta\cos\theta$	0	0	$-\sin\theta\cos\theta$	$\sin^2 \theta$	0	0	0	0	0
(13)	0	0	0	0	0	$\sin \theta \cos \theta$	$\frac{1}{2}(\cos 2\theta + \cos \phi)$	$-\frac{1}{2}\sin\phi$	$-\frac{1}{2}\sin\phi$	$\frac{1}{2}(\cos 2\theta - \cos \phi)$	$-\sin\theta\cos\theta$	0	0	0	0	0
(14)	0	0	0	0	0	0	$\frac{1}{2} \sin \phi$	$\cos^2 \frac{\phi}{2}$	$-\sin^2\frac{\phi}{2}$	$-\frac{1}{2}\sin\phi$	0	0	0	0	0	0
(23)	0	0	0	0	0	0	$\frac{1}{2} \sin \phi$	$-\sin^2 \frac{\phi}{2}$	$\cos^2 \frac{\phi}{2}$	$-\frac{1}{2}\sin\phi$	0	0	0	0	0	0
(24)	0	0	0	0	0		$\frac{1}{2}(\cos 2\theta - \cos \phi)$	$\frac{1}{2} \sin \phi$	$\frac{1}{2} \sin \phi$	$\frac{1}{2}(\cos 2\theta + \cos \phi)$	$-\sin\theta\cos\theta$	0	0	0	0	0
(34)	0	0	0	0	0	$\sin^2 \theta$	$\sin \theta \cos \theta$	0	0	$\sin \theta \cos \theta$	$\cos^2 \theta$	0	0	0	0	0
(123)	0	$\frac{1}{2}i \sin \theta \sin \phi$	$-i \sin \theta \sin^2 \frac{\phi}{2}$	$-i\cos\theta\sin^2\frac{\phi}{2}$	$-\frac{1}{2}i\cos\theta\sin\phi$	0	0	0	0	0	0	$\cos \theta \cos^2 \frac{\phi}{2}$	$-\frac{1}{2}\cos\theta\sin\phi$	$\frac{1}{2} \sin \theta \sin \phi$	$\sin \theta \cos^2 \frac{\phi}{2}$	0
(124)	0	$i \sin \theta \sin^2 \frac{\phi}{2}$	$\frac{1}{2}i \sin \theta \sin \phi$	$\frac{1}{2}i\cos\theta\sin\phi$	$-i\cos\theta\sin^2\frac{\phi}{2}$	0	0	0	0	0	0	$\frac{1}{2}\cos\theta\sin\phi$	$\cos \theta \cos^2 \frac{\phi}{2}$	$-\sin\theta\cos^2\frac{\phi}{2}$	$\frac{1}{2} \sin \theta \sin \phi$	0
(134)	0	$-i\cos\theta\sin^2\frac{\phi}{2}$	$-\frac{1}{2}i\cos\theta\sin\phi$	$\frac{1}{2}i \sin \theta \sin \phi$	$-i \sin \theta \sin^2 \frac{\phi}{2}$	0	0	0	0	0	0	$\frac{1}{2} \sin \theta \sin \phi$	$\sin \theta \cos^2 \frac{\phi}{2}$	$\cos \theta \cos^2 \frac{\phi}{2}$	$-\frac{1}{2}\cos\theta\sin\phi$	0
(234)	0	$\frac{1}{2}i\cos\theta\sin\phi$	$-i\cos\theta\sin^2\frac{\phi}{2}$	$i \sin \theta \sin^2 \frac{\phi}{2}$	$\frac{1}{2}i \sin \theta \sin \phi$	0	0	0	0	0	0	$-\sin\theta\cos^2\frac{\phi}{2}$	$\frac{1}{2} \sin \theta \sin \phi$	$\frac{1}{2}\cos\theta\sin\phi$	$\cos \theta \cos^2 \frac{\phi}{2}$	0
(1234)	0	0	0	0	0	0	0	0	0	0	0	0	0	0	0	1

FIG. 3. The Superoperator Matrix  $\hat{\mathcal{U}}$  for the 2-qubit  $fSim(\theta,\phi)$  Gate. If  $\phi=0$ , this is an  $XY(\theta)$  gate with a block-diagonal compound PL matrix. If  $\theta=0, \phi=\pi$  it is monomial, with entries from  $\{\pm 1, \pm i\}$ . If  $\theta\neq 0, \phi=\pi$ , the gate is of the form  $\hat{\mathcal{W}}=\hat{\mathcal{U}}\circ\hat{\mathcal{V}}$  discussed in Section V.

Hence  $\mathbb{E}(m)$  is bounded as:

$$\mathbb{E}(m) \leq l \cdot \mathbb{E}(m_{\mu})$$

$$\leq l + \frac{1}{2^{2n}} \sum_{\mu} \frac{4 \ln(4/\delta)}{\epsilon^{2}}$$

$$\leq 1 + \frac{1}{\epsilon^{2}\delta} + \frac{\#[\chi_{\mathcal{U}}(I, J) \neq 0]}{2^{2n}} \frac{4 \ln(4/\delta)}{\epsilon^{2}},$$
(B8)

Where  $\#[\chi_{\mathcal{U}}(I,J)\neq 0]$  is the number of non-zero elements in the superoperator matrix  $\hat{\mathcal{U}}$ . From Theorem 1 we know this to be  $\leq 2^{4n}/\sqrt{n}$  for all MGs, giving the general bound stated in the main text. However, if R has a particular structure we can bound  $\mathbb{E}(m)$  further. For example, if R is a 2D rotation, i.e.  $R=\mathrm{diag}(\mathbb{1}_{k-2},R_{[2\times 2]},\mathbb{1}_{2n-k})$ , then  $\#[\chi_{\mathcal{U}}(I,J)\neq 0]=\frac{3}{2}2^{2n}$ , leading to a bound independent of both n and  $\theta$ . Thus, in some cases (i.e. when  $\alpha\ll 1$ ) it may be preferable to use the general bound to determine l and  $m_{\mu}$ .

### 2. Well-conditioned Case

From the properties of compound matrices it follows that  $\hat{\mathcal{U}}$  is an orthogonal matrix, hence its elements  $|\chi_{\mathcal{U}}(I,J)| \leq 1$  (in fact, this is true for all superoperators). If we are in knowledge of the well-conditioning parameter  $\alpha$ , such that all non-zero elements  $|\chi_{\mathcal{U}}(I,J)| \geq \alpha$ , when we can use the Hoeffding inequality for both bounds, leading to a bound for m independent of system size. When finding l, from the above discussion it follows that the summands  $Z_{\mu} = \frac{1}{l} X_{\mu}$  in  $Y = \sum_{\mu} Z_{\mu}$  are bounded as  $|Z_{\mu}| \leq \frac{1}{\alpha l}$ . Hence,

$$C = \sum_{u=1}^{l} \frac{4}{\alpha^2 l^2} = \frac{4}{\alpha^2 l}.$$
 (B9)

Choosing  $l = \lceil 2 \ln(2/\delta)/\alpha^2 \epsilon^2 \rceil$  then ensures the RHS of Hoeffding's inequality equals  $\delta$ . The expression for  $m_{\mu}$  remains the same, and we can use the well-conditioned property againt to show that  $m_{\mu} \leq 1 + 2 \ln(2/\delta)/\alpha^2 \epsilon^2 l$ , and thus  $m \leq 4 \ln(2/\delta)/\alpha^2 \epsilon^2$ .

# Appendix C: Strategies for Large Numbers of Qubits

Here we give some guidance on how to calculate  $\hat{\mathcal{U}}$  for larger MG circuits. To do this, we first restate the following theorem [23]:

**Theorem 2.** For any  $R \in SO(n)$ , there exists a set of generalised Euler angles  $\{\theta_j^k\}_{1 \leq j \leq k \leq n-1}$ , where:

$$1 \le k \le n - 1, \qquad 1 \le j \le k, \tag{C1}$$

with

$$0 \leq \theta_1^k < 2\pi, \qquad \quad 0 \leq \theta_j^k < \pi \ \ \textit{for} \ j \neq 1.$$

R is then given by:

$$R = R^{(n-1)} \cdots R^{(1)},$$
 (C2)

where

$$R^{(k)} = R_1(\theta_1^k) \cdots R_k(\theta_k^k), \tag{C3}$$

and

$$R_k(\theta) = \begin{pmatrix} \mathbb{1}_{k-1} & & & \\ & \cos \theta & \sin \theta & \\ & -\sin \theta & \cos \theta & \\ & & \mathbb{1}_{n-k-1} \end{pmatrix}$$
 (C4)

The Euler angles are unique, except when some  $\theta_j^k$  is 0 or  $\pi$  (for  $j \geq 2$ ).

*Proof.* We will prove this by induction. The result is true for n = 2; assume it holds for the case of SO(n-1). Then, consider  $R^{(n-1)}$  acting on the  $n^{\text{th}}$  unit vector  $|n\rangle$ :

$$R^{(n-1)}|n\rangle = R_1(\theta_1^{n-1}) \cdots R_{n-1}(\theta_{n-1}^{n-1})|n\rangle$$

$$= \cos(\theta_{n-1}^{n-1})|n\rangle$$

$$+ \sin(\theta_{n-1}^{n-1})\cos(\theta_{n-2}^{n-1})|n-1\rangle$$

$$+ \cdots$$

$$+ \sin(\theta_{n-1}^{n-1}) \cdots \sin(\theta_2^{n-1})\cos(\theta_1^{n-1})|2\rangle$$

$$+ \sin(\theta_{n-1}^{n-1}) \cdots \sin(\theta_2^{n-1})\sin(\theta_1^{n-1})|1\rangle$$

Which is the unique representation of a point in  $\mathbb{R}^n$  in spherical coordinates. Hence,

$$R^{(n-1)}|n\rangle = R|n\rangle,$$

and so

$$(R^{(n-1)})^{-1}R = \begin{pmatrix} \tilde{R} & 0 \\ 0 & 1 \end{pmatrix},$$

and by the induction hypthesis  $\tilde{R}$  belongs to SO(n-1). Hence, we can obtain R by multiplying both sides by  $R^{(n-1)}$ .

We can use this procedure in reverse to obtain the angles  $\{\theta_j^k\}$  for a given R. First, solve for  $\{\theta_j^{n-1}\}$ 's using the rightmost column of the matrix. Then, left-multiply by  $(R^{(n-1)})^{-1} = R_{n-1}(-\theta_{n-1}^{n-1}) \cdots R_1(-\theta_1^1)$ , solve for  $\{\theta_j^{n-2}\}$ 's, and repeat until all of the Euler angles are found. Other methods also exist, such as the algorithm of Hoffman et al. [24].

We may also use a few important properties of compound matrices [25, 26]:

**Theorem 3.** Let A and B be  $n \times n$  matrices. The following statements are true:

- $C_r(AB) = C_r(A)C_r(B)$  (Cauchy-Binet Formula);
- $C_r(A^{\dagger}) = C_r(A)^{\dagger};$
- If det  $A \neq 0$ , then  $C_r(A^{-1}) = C_r(A)^{-1}$ ;
- If A is: Triangular, Diagonal, Orthogonal, Unitary, (Anti-) Symmetric, (Anti-) Hermitian, or Positive (semi-) definite, then so is  $C_r(A)$ .

From the above two theorems, it follows that any MG superoperator can be written as the product of n(2n-1) MG superoperators:

$$\hat{\mathcal{U}} = \hat{\mathcal{U}}^{(2n-1)} \cdots \hat{\mathcal{U}}^{(1)}, \tag{C5}$$

with each  $\hat{\mathcal{U}}^{(k)}$  given by:

$$\hat{\mathcal{U}}^{(k)} = \hat{\mathcal{U}}_1(\theta_1^k) \cdots \hat{\mathcal{U}}_k(\theta_k^k). \tag{C6}$$

Here,  $\hat{\mathcal{U}}_k(\theta)$  is a block-diagonal matrix of compound matrices of  $R_k(\theta)$ :

$$\hat{\mathcal{U}}_k(\theta) = \bigoplus_{i=0}^{2n} C_i(R_k(\theta)). \tag{C7}$$

Each  $\hat{\mathcal{U}}_k(\theta)$  is a  $2^{2n} \times 2^{2n}$  matrix, and we will show that it contains at most  $\frac{3}{2}2^{2n}$  non-zero elements, which

we can generate using simple rules. Furthermore, it is diagonal for  $\theta = 0, \pi$ , so in practice one can compute  $\hat{\mathcal{U}}$  as well as  $\alpha$  using the following procedure:

- 1. From R, find the Euler Angles  $\{\theta_i^k\}$ .
- 2. For each  $\theta_j^k$ , generate the non-zero elements of  $\hat{\mathcal{U}}_k(\theta_j^k)$ .
- 3. Using sparse matrix multiplication methods, perform at most n(2n-1) matrix multiplications to obtain  $\hat{\mathcal{U}}$ .
- 4. (Optional) Find  $\alpha$  from the non-zero elements of  $\hat{\mathcal{U}}$  using a sorting algorithm.

We end this section with the rule for generating non-zero elements of  $\hat{\mathcal{U}}_k(\theta)$ :

**Theorem 4.** The matrix elements  $\chi_{\mathcal{U}_k}(I,J)$  of  $\hat{\mathcal{U}}_k(\theta)$  satisfy the following:

- If  $I = \emptyset$  or  $I = \{1, \dots, 2n\}$ , then  $\chi_{\mathcal{U}_k}(I, I) = 1$ ;
- If |I| = |J| = 1, i.e.  $I = \{i\}$ ,  $J = \{j\}$ , then  $\chi_{\mathcal{U}_k}(I, J) = [R_k(\theta)]_{ij}$ ;
- If  $I \ni k$  and  $I \ni k+1$ , or  $I \not\ni k$  and  $I \not\ni k+1$ , then  $\chi_{\mathcal{U}_k}(I,I)=1$ ;
- If  $I \ni k$  and  $I \not\ni k+1$ , or  $I \not\ni k$  and  $I \ni k$ , then  $\chi_{\mathcal{U}_k}(I,I) = \cos \theta$ ;
- If I < J (in lexicographic ordering), and I, J differ on only one index (so that  $I \ni k, I \not\ni k+1$  and  $J \not\ni k, J \ni k+1$ ), then  $\chi_{\mathcal{U}_k}(I, J) = \sin \theta$ ;
- If I > J, and I, J differ on only one index (so that  $I \not\ni k, I \ni k+1$  and  $J \ni k, J \not\ni k+1$ ), then  $\chi_{\mathcal{U}_k}(I, J) = -\sin\theta$ ;
- In all other cases,  $\chi_{\mathcal{U}_k}(I,J) = 0$ .

*Proof.* All cases can be easily verified by considering the different structures of submatrices formed when rows in I,J are preserved, and calculating their determinants. Counting the number of non-zero elements, we also get

$$\#[\chi_{\mathcal{U}_k}(I,J) = 1] = \frac{1}{2}2^{2n}$$
$$\#[\chi_{\mathcal{U}_k}(I,J) = \cos\theta] = \frac{1}{2}2^{2n}$$
$$\#[\chi_{\mathcal{U}_k}(I,J) = \pm\sin\theta] = \frac{1}{4}2^{2n}$$

Giving at most  $\frac{3}{2}2^{2n}$  non-zero elements.

[1] R. Jozsa and A. Miyake, Matchgates and classical simulation of quantum circuits, Proceedings of the Royal Society A: Mathematical, Physical and Engineering Sciences 464, 3089 (2008).

- [2] L. G. Valiant, Quantum circuits that can be simulated classically in polynomial time, SIAM Journal on Computing 31, 1229 (2002), https://doi.org/10.1137/S0097539700377025.
- [3] E. Knill, Fermionic linear optics and matchgates (2001), arXiv:quant-ph/0108033 [quant-ph].
- [4] B. M. Terhal and D. P. DiVincenzo, Classical simulation of noninteracting-fermion quantum circuits, Physical Review A 65, 10.1103/physreva.65.032325 (2002).
- [5] D. P. DiVincenzo and B. M. Terhal, Fermionic linear optics revisited, Foundations of Physics 35, 1967 (2005).
- [6] S. Bravyi, Contraction of matchgate tensor networks on non-planar graphs (2008), arXiv:0801.2989 [quant-ph].
- [7] A. Sørensen and K. Mølmer, Entanglement and quantum computation with ions in thermal motion, Physical Review A 62, 10.1103/physreva.62.022311 (2000).
- [8] B. Foxen, C. Neill, A. Dunsworth, P. Roushan, B. Chiaro, A. Megrant, J. Kelly, Z. Chen, K. Satzinger, R. Barends, F. Arute, K. Arya, R. Babbush, D. Bacon, J. Bardin, S. Boixo, D. Buell, B. Burkett, Y. Chen, R. Collins, E. Farhi, A. Fowler, C. Gidney, M. Giustina, R. Graff, M. Harrigan, T. Huang, S. Isakov, E. Jeffrey, Z. Jiang, D. Kafri, K. Kechedzhi, P. Klimov, A. Korotkov, F. Kostritsa, D. Landhuis, E. Lucero, J. McClean, M. McEwen, X. Mi, M. Mohseni, J. Mutus, O. Naaman, M. Neeley, M. Niu, A. Petukhov, C. Quintana, N. Rubin, D. Sank, V. Smelyanskiy, A. Vainsencher, T. White, Z. Yao, P. Yeh, A. Zalcman, H. Neven, and J. M. and, Demonstrating a continuous set of two-qubit gates for near-term quantum algorithms, Physical Review Letters 125, 10.1103/physrevlett.125.120504 (2020).
- [9] Y. Sung, L. Ding, J. Braumüller, A. Vepsäläinen, B. Kannan, M. Kjaergaard, A. Greene, G. O. Samach, C. McNally, D. Kim, et al., Realization of high-fidelity cz and z z-free iswap gates with a tunable coupler, Physical Review X 11, 021058 (2021).
- [10] D. M. Abrams, N. Didier, B. R. Johnson, M. P. d. Silva, and C. A. Ryan, Implementation of xy entangling gates with a single calibrated pulse, Nature Electronics 3, 744 (2020).
- [11] M. Kjaergaard, M. E. Schwartz, J. Braumüller, P. Krantz, J. I.-J. Wang, S. Gustavsson, and W. D. Oliver, Superconducting qubits: Current state of play, Annual Review of Condensed Matter Physics 11, 369–395 (2020).
- [12] S. M. Young, N. T. Jacobson, and J. R. Petta, Optimal control of a cavity-mediated iSWAP gate between silicon spin qubits, Phys. Rev. Appl. 18, 064082 (2022).

- [13] N. Grzesiak, R. Blümel, K. Wright, K. M. Beck, N. C. Pisenti, M. Li, V. Chaplin, J. M. Amini, S. Debnath, J.-S. Chen, et al., Efficient arbitrary simultaneously entangling gates on a trapped-ion quantum computer, Nature communications 11, 2963 (2020).
- [14] J. Helsen, S. Nezami, M. Reagor, and M. Walter, Matchgate benchmarking: Scalable benchmarking of a continuous family of many-qubit gates, Quantum 6, 657 (2022).
- [15] J. Claes, E. Rieffel, and Z. Wang, Character randomized benchmarking for non-multiplicity-free groups with applications to subspace, leakage, and matchgate randomized benchmarking, PRX Quantum 2, 010351 (2021).
- [16] J. Kempe, D. Bacon, D. P. DiVincenzo, and K. B. Whaley, Encoded universality from a single physical interaction (2001), arXiv:quant-ph/0112013 [quant-ph].
- [17] S. T. Flammia and Y.-K. Liu, Direct fidelity estimation from few pauli measurements, Physical Review Letters 106, 10.1103/physrevlett.106.230501 (2011).
- [18] M. A. Nielsen, A simple formula for the average gate fidelity of a quantum dynamical operation, Physics Letters A 303, 249 (2002).
- [19] A. Chapman and A. Miyake, Classical simulation of quantum circuits by dynamical localization: Analytic results for pauli-observable scrambling in time-dependent disorder, Physical Review A 98, 10.1103/physreva.98.012309 (2018).
- [20] A. Chapman and S. T. Flammia, Fermionic averaged circuit eigenvalue sampling (2025), arXiv:2504.01936 [quant-ph].
- [21] J. Burkat, Matchgate benchmarking github repository (2024).
- [22] M. Oszmaniec, N. Dangniam, M. E. Morales, and Z. Zimborás, Fermion sampling: A robust quantum computational advantage scheme using fermionic linear optics and magic input states, PRX Quantum 3, 020328 (2022).
- [23] E. S. Meckes, The Random Matrix Theory of the Classical Compact Groups, Cambridge Tracts in Mathematics (Cambridge University Press, 2019).
- [24] D. K. Hoffman, R. C. Raffenetti, and K. Ruedenberg, Generalization of Euler Angles to N-Dimensional Orthogonal Matrices, Journal of Mathematical Physics 13, 528 (1972).
- [25] C. Kravvaritis and M. Mitrouli, Compound matrices: properties, numerical issues and analytical computations, Numerical Algorithms 50, 155 (2009).
- [26] K. Nambiar and S. Sreevalsan, Compound matrices and three celebrated theorems, Mathematical and Computer Modelling 34, 251 (2001).